Macromolecules

ARTICLE

pubs.acs.org/Macromolecules

Cooperative Dynamics in Polystyrene and Low-Mass Molecule Mixtures

Shogo Nobukawa,*,† Osamu Urakawa,* Toshiyuki Shikata, and Tadashi Inoue

Department of Macromolecular Science, Graduate School of Science, Osaka University, Toyonaka, Osaka 560-0043, Japan

ABSTRACT: We conducted dielectric and viscoelastic relaxation measurements for polystyrene (PS)/4-pentyl-4′-cyanobiphenyl (5CB) and PS/4-pentyl-4″-cyanoterphenyl (5CT) mixtures in the miscible state with the weight fractions of 5CB or 5CT from 0.04 to 0.27 to examine the relationship between two-component dynamics in the mixture. Dielectric relaxation measurements mainly probed the dynamics of low-mass molecule (LM), 5CB or 5CT, because of the much larger dipole moment of LMs compared to that of PS. PS/5CB mixtures exhibited bimodal dielectric relaxation, while PS/5CT showed unimodal relaxation. The observed two relaxation modes (slow and fast modes) in PS/5CB were attributed to the full rotational motion and partial rotational motion of 5CB, respectively. The latter motion is allowed in the restricted space surrounded by less mobile PS matrix. In the case of 5CT, the fast mode was suppressed due to the larger size of 5CT molecule, and only the slow mode (rotational mode) appeared. The relaxation times of slow mode for 5CB and 5CT had approximately the same (non-Arrhenius-type) temperature dependence with the viscoelastic relaxation time for the terminal flow zone of PS at high temperatures (at least 20−30 K higher than the glass transition temperature). This result suggested that the slow modes of 5CB and 5CT are cooperative with a global motion of PS-chain. In contrast, relaxation time for the fast mode observed in PS/5CB had weaker (Arrhenius-type) temperature dependence than the slow mode, which indicated that the fast mode of 5CB is decoupled with the PS chain motion.

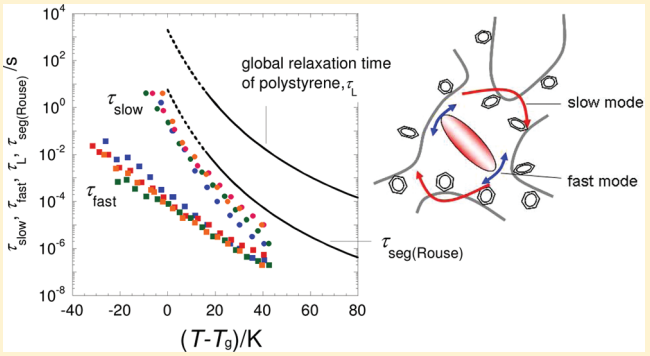

1. INTRODUCTION

The glass transition phenomena of polymers, low-mass molecules (LMs), and their mixtures have been studied so far for many years.[1−15] It is now widely accepted that the glass transition is not thermodynamical transition but kinetic transition. In polymers, approaching the glass transition temperature T_g from above makes the micro-Brownian motion of the chain backbone slow down. This process can be monitored by several dynamic methods such as mechanical and dielectric measurements. In the case of dielectric measurements, the major relaxation observed in the vicinity of T_g is called "α relaxation" or "segmental relaxation".[16,17]

Addition of LMs into polymers usually makes the glass transition temperature T_g decrease since LMs generally have much lower T_g than polymers: this is referred to as "plasticization".[4] LMs practically used as plasticizers should not be volatile (should have high boiling points) and thus have relatively large molecular sizes (e.g., di-*n*-butyl phthalate, tricresyl phosphate, and so on). Since single but broad glass transition for such plasticized polymers has been often observed, the molecular motion of polymers such as α (segmental) motion and the rotational motion of LMs are thought to be cooperative.

Fluorescent LMs dissolved in polymers have been often used to probe the dynamical environment of polymer matrices especially in order to study the glass transition phenomena. Such probe methods are premised on the cooperativity between motions of the polymers and LMs. However, it is not always the case that the two-component motions are cooperative. There are some miscible mixture systems which exhibit decoupling of two-component motions: e.g., Adachi et al. studied temperature dependence of the complex dielectric constant for polystyrene (PS)/toluene mixture and reported that two dielectric loss peaks corresponding to the segmental motion of PS and the rotational motion of toluene appeared in different temperature region. The similar behavior is also seen in miscible polymer−polymer mixtures when the two components have largely separated T_gs.[12,18−20] Such decoupling phenomena of the component dynamics is called "dynamic heterogeneity". In systems with high dynamic asymmetry (both polymer−LM and polymer−polymer mixtures), broad glass transition observed by calorimetric measurements can be sometimes resolved into two-component contributions.[14,15]

Urakawa et al. studied molecular size effect on the dynamic heterogeneity in the mixture of PS and several LMs through dielectric relaxation measurements.[12,18,19] They found that the rotational relaxation of LM appeared near the calorimetric T_g when the LM size became comparable to the Kuhn segmental size of PS. By assuming that α (segmental) motion of PS should take place in the vicinity of T_g for the mixtures with high PS

Received: July 25, 2011
Revised: September 6, 2011
Published: September 21, 2011

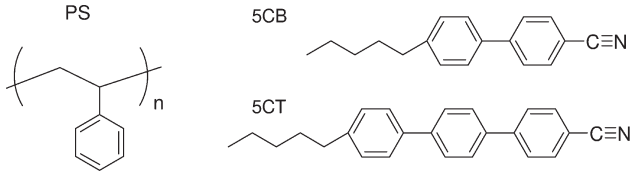

Figure 1. Chemical structures of polystyrene (PS), 4-pentyl-4′-cyanobiphenyl (5CB), and 4-pentyl-4′-cyanoterphenyl (5CT).

content, they concluded that α-motion and LM motion became cooperative for LMs with comparable or larger size than the Kuhn length of the polymers. Since α-relaxation of PS could not be dielectrically observed due to its small dipole moment, the above-mentioned assumption was necessary to deduce that conclusion. Similar study was made by van den Berg et al.[21] and Hains and Williams,[22] in which polymer motion was implicitly assumed to be cooperative with LM motion. According to Urakawa's result, the reason for dynamic heterogeneity in PS/toluene mixture can be attributed to the small size of toluene molecule compared to the Kuhn length of PS. In this study, we aim to clarify whether the both motions are really cooperative or not in two PS/LM mixtures—PS/5CB and PS/5CT—through the examination of the temperature dependence of the component relaxation times. As described previously, due to much lower dielectric relaxation (DR) intensity of PS than that of LMs, the DR method is a powerful tool to selectively observe the LM dynamics. In contrast, viscoelastic relaxation (VR) in the terminal region reflects only the response from polymer component, so that VR measurements can be used to evaluate the PS component dynamics. By conducting both measurements, the two component motion in the mixture can be clarified. From the comparison of the obtained DR time of LMs with the VR time (terminal relaxation time) of PS and also with the calculated relaxation time for the Rouse segment unit from the VR time, dynamic cooperativeity of the two components was examined. Furthermore, the dependence of the DR time of LMs on the molecular sizes will also be discussed.

2. EXPERIMENTAL SECTION

2.1. Samples. Polystyrene (PS, Figure 1) was synthesized by living anionic polymerization of styrene (Wako Pure Chemical Industries, Ltd.) in benzene using *sec*-butyllithium (Sigma-Aldrich) as an initiator. The weight-average molecular weight (M_w) and molecular weight distribution index (M_w/M_n) of PS were determined to be 15.9×10^3 and 1.07, respectively, by gel-permeation chromatography (GPC) using PS standard samples (Tosoh). Two LM samples, 4-pentyl-4′-cyanobiphenyl (5CB, Figure 1, purity >97%) and 4-pentyl-4′′-cyanoterphenyl (5CT, Figure 1, purity >97%), were purchased from Wako Pure Chemical Industries, Ltd., and used as received. PS/5CB and PS/5CT mixtures were prepared by the freeze-drying method from a benzene solution and subsequent removal of the residual solvent at an elevated temperature (100−150 °C) in vacuo. We confirmed that all samples were transparent and thus homogeneously mixed.

The weight fractions of 5CB and 5CT in the mixtures, W_{5CB} and W_{5CT}, were determined just before the dielectric or viscoelastic measurement, from the integrated ^{1}H NMR intensities of the corresponding component signals measured with Excalibur-270 (JEOL Ltd., Tokyo, Japan) for the deuteriochloroform solutions of the mixtures. The obtained values are listed in Table 1.

2.2. Measurements. Dielectric relaxation (DR) measurements of the PS/5CB and PS/5CT mixtures at various temperatures (−25 to 150 °C) were carried out by using two LCR meters, 4284A (Hewlett-Packard, angular frequency $\omega = 1.26 \times 10^2 - 5.03 \times 10^6$ s^{-1}) and 7600 (Quad Tech, $\omega = 62.8 - 1.26 \times 10^7$ s^{-1}), and a homemade apparatus consisting of a Current Amplifier 428 (Keithley) and a fast Fourier transform (FFT) analyzer VC-2440 (Hitachi, Japan) which covers the frequency range of $\omega = 1.57 \times 10^{-2} - 6.28 \times 10^3$ s^{-1}. Samples were set in parallel plate electrode cell with a glass spacer. After annealing at T_g + 50 K in vacuo for 2 h, dielectric measurements were carried out.

Dynamic viscoelastic relaxation (VR) measurements were performed above the T_g of mixtures with two dynamic stress rheometers (SR-500R, or SR-200, Rheometrics Inc.) using 25 mm parallel plates fixture after the DR measurement.

The glass transition temperature T_g of each mixture was determined by differential scanning calorimetry (DSC 6220, EXSTAR-6000, Seiko Instruments Inc., Japan) in the heating process with a rate of 10 K min^{-1}. For all the samples, the T_g values were checked to be unchanged before and after the DR and VR measurements to confirm that the composition did not change during the measurement.

Table 1. Weight Fractions of Low-Mass Components (W_{5CB}, W_{5CT}), Glass Transition Temperatures (T_g), Dielectric Relaxation Intensities, $\Delta\varepsilon$, and Activation Energies, E_a, in PS/5CB or PS/5CT Mixtures

code	W_{5CB} or W_{5CT}	T_g/K	$\Delta\varepsilon_{theo}$ [a]	$\Delta\varepsilon_{total}$ [b]	$\Delta\varepsilon_{slow}$ [b]	$\Delta\varepsilon_{fast}$ [b]	E_a/kJ mol^{-1}
PS		373	0.039	0.04			126[c]
PS/5CB	0.067	348	0.72	0.90	0.40	0.50	180[d]
	0.13	331	1.34	1.35	0.35	1.00	135[d]
	0.19	319	2.10	2.08	0.48	1.60	130[d]
	0.27	301	3.35	3.58	0.64	2.94	124[d]
PS/5CT	0.040	364	0.31	0.37			
	0.11	352	0.95	0.75			

[a] Theoretical values were calculated by Onsager's theory represented by eq 5 at T_g + 20 K for each mixture. [b] These values were obtained by fitting with eq 6 at T_g + 20 K. [c] β-relaxation of PS. [d] Fast relaxation mode of 5CB.

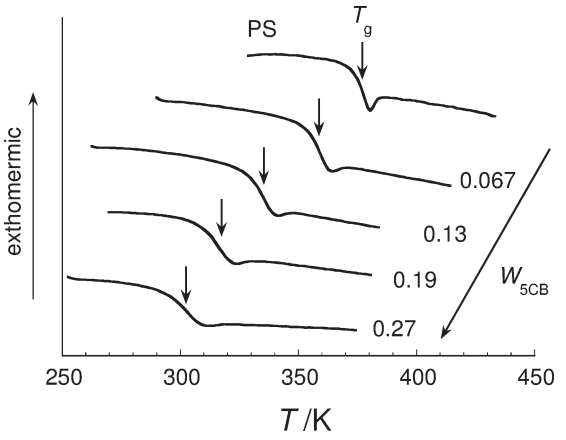

Figure 2. DSC curves of bulk PS and PS/5CB mixtures at various compositions. The numbers represent the weight fractions of 5CB, W_{5CB}. The glass transition temperature, T_g, is indicated by the arrows.

3. RESULTS AND DISCUSSION

3.1. Composition Dependence of Glass Transition Temperature. Figure 2 shows DSC traces for bulk PS and PS/5CB mixtures. For all samples, a single glass transition was observed as already reported by Hori et al.[23] Judging from the reproducibility

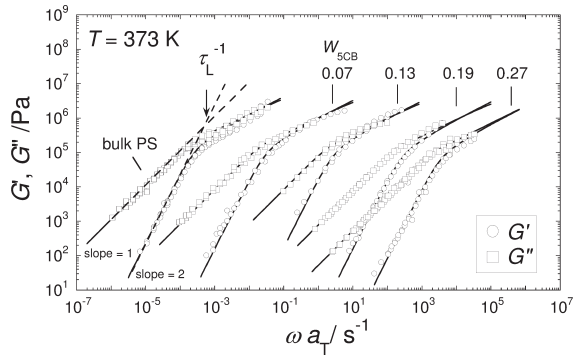

Figure 3. Composite curves of bulk PS and PS/5CB mixtures at 373 K. Solid lines are the fitted results by eqs 1−3. Dotted lines on G' and G'' data represent the power law relations: $G' \sim \omega^2$ and $G'' \sim \omega^1$.

of the DSC data and also the transparency of all samples, we regarded PS/5CB mixtures to be homogeneously mixed without undergoing phase separations. The glass transition temperature, T_g, was determined from the inflection point of the curve as indicated by arrows in Figure 2. Table 1 summarizes T_gs of PS/5CB and PS/5CT mixtures. It is seen that T_g decreases with increasing 5CB or 5CT concentration, meaning that these LMs work as ordinary plasticizers. Since the T_g of PS/5CB was lower than that of PS/5CT at the same composition, the ability of plasticization of 5CB is stronger than that of 5CT.

3.2. Viscoelastic Relaxation Behavior of PS/5CB and PS/5CT Mixtures. Figure 3 displays the composite curves of the complex shear modulus, $G^*(\omega) = G'(\omega) + iG''(\omega)$ for bulk PS and PS/5CB mixtures at the reference temperature of 373 K. $G'(\omega)$ and $G''(\omega)$ are storage and loss moduli, respectively. The method of reduced variables[4] worked well for all the systems in the temperature range examined here. Since molecular weight of PS is 15.9×10^3 being lower than the entanglement molecular weight ($M_e \sim 20\,000$), the obtained viscoelastic curves are compared with the Rouse model,[24] which is known to reproduce the viscoelastic relaxation spectra very well for nonentangled polymers. This model assumes a polymer chain composed of $N + 1$ beads linearly connected with N springs and the Brownian force acting on each bead. The expression for G' and G'' is given by

$$G'(\omega) = \frac{cRT}{M}\sum_p^N \frac{(\omega\tau_p)^2}{1 + (\omega\tau_p)^2} \quad (1)$$

$$G''(\omega) = \frac{cRT}{M}\sum_p^N \frac{\omega\tau_p}{1 + (\omega\tau_p)^2} \quad (2)$$

Here, c, R, T, and M are the polymer concentration, gas constant, absolute temperature, and polymer molecular weight, respectively. The relaxation time of the pth normal (Rouse) mode, τ_p, is given by

$$\tau_p = \frac{\tau_1}{p^2} = \frac{\zeta b^2 N^2}{6\pi^2 p^2 k_B T} \quad (3)$$

Here, ζ, b, N, and k_B are friction factor, effective bond length, number of the Rouse segments, and the Boltzmann constant, respectively. Particularly, τ_1 is the longest relaxation time approximately given by the terminal relaxation time, τ_L, for narrow molecular weight distribution polymers. Furthermore, the fastest mode corresponding to the case of $p = N$ in eqs 1 and 2 is the fundamental process for the Rouse dynamics, that is, the relaxation

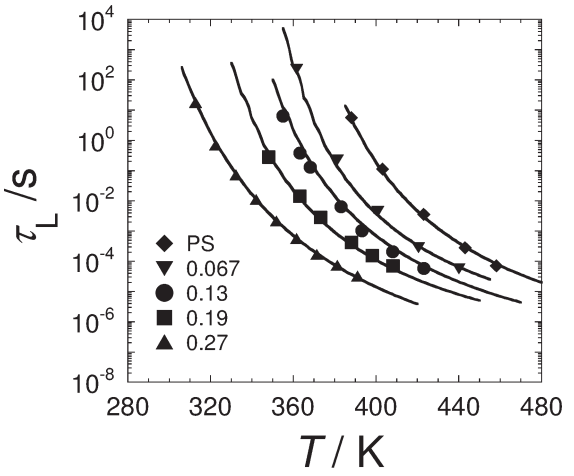

Figure 4. Temperature dependence of τ_L for PS and PS/5CB at various compositions. Solid curves represent the fitted results by using the WLF equation given by eq 4.

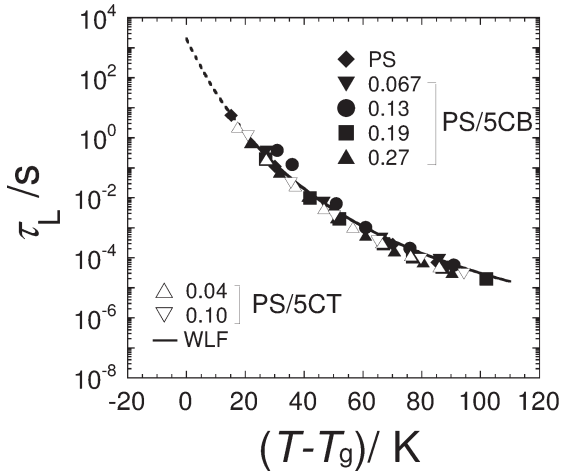

Figure 5. Dependence of τ_L on $T - T_g$. A solid line is a curve calculated from the WLF equation (eq 4) with $c_1 = 12.5$, $c_2 = 60$ K, and $T_r = T_g$.

of the Rouse segment unit. The fastest relaxation time, τ_N, is given as τ_1/N^2 from eq 3. As seen in Figure 3, the G' and G'' curves were well fitted by the Rouse model (solid lines) with τ_1 as an only parameter. The terminal relaxation time, τ_L, was determined from the crossing frequency of two power law lines, $G'(\omega) \propto \omega^2$ and $G''(\omega) \propto \omega^1$, as shown by the dotted lines in Figure 3, and we found $\tau_L \approx \tau_1$.

Figure 4 illustrates the temperature dependence of τ_L for PS and PS/5CB at various compositions. With increasing 5CB concentration, τ_L curve shifts to lower temperatures, reflecting the decrease of the friction factor due to the decrease of T_g. In Figure 5, τ_L values are plotted against temperature difference, $T - T_g$. All the τ_L values overlap and can be expressed by a single universal curve as a function of $T - T_g$. In Figures 4 and 5, the solid lines represent calculated results with the following Williams−Landel−Ferry (WLF) equation.[25]

$$\log(\tau_L(T)/\tau_L(T_g)) = -\frac{c_1(T - T_g)}{c_2 + T - T_g} \quad (4)$$

Here, c_1 and c_2 are constants and approximately regarded to be independent of concentration. The obtained c_1 and c_2 values

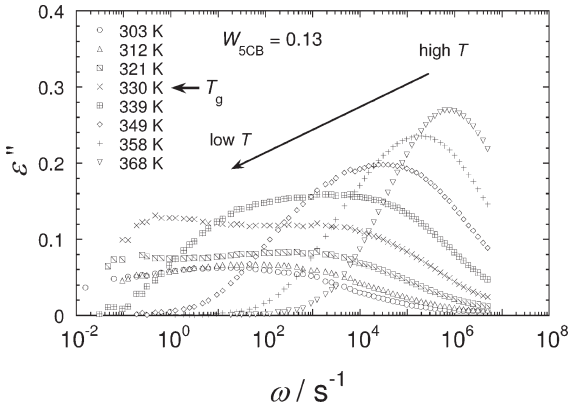

Figure 6. Angular frequency dependence of dielectric loss, ε'', for PS/5CB (W_{5CB} = 0.13) at various temperatures.

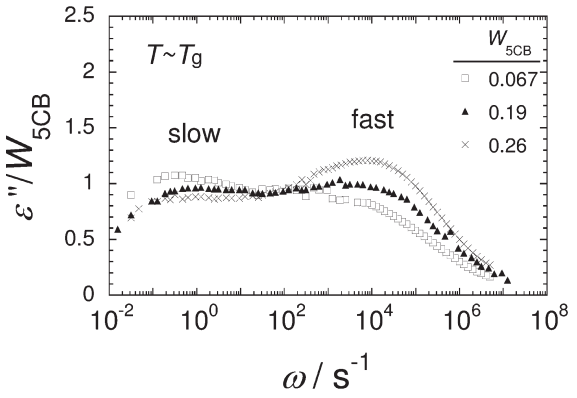

Figure 7. Comparison of dielectric spectra for PS/5CB mixtures at various compositions. The vertical axis is reduced by the weight fraction of 5CB, W_{5CB}, for each mixture. With increasing W_{5CB}, intensity of the slow component becomes weaker while the fast component becomes stronger.

were c_1 = 12 and c_2 = 60 K, which are not so different from the reported general vales, c_1 = 17.44 and c_2 = 51.6 K.[26]

3.3. Dielectric Relaxation Behavior of PS/5CB Mixtures. Figure 6 shows the angular frequency, ω, dependence of dielectric losses, ε'', for PS/5CB mixture with W_{5CB} = 0.13 at several temperatures. With decreasing temperature, the dielectric spectra become broader. This indicates the breakdown of time−temperature superposition (TTS) principle for ε'' curves of the PS/5CB mixture. In addition to that, the ε'' spectra exhibit bimodal distribution particularly in the vicinity of and below the T_g. Mixtures with different compositions (W_{5CB} = 0.067, 0.19, and 0.27) also showed the similar trend concerning the temperature dependence of the spectrum shape.

Figure 7 compares the ε'' spectra for PS/5CB mixtures with various compositions around the T_g of each mixture. In this figure, ε'' reduced by W_{5CB} (ε''/W_{5CB}) are compared since, as will be discussed in detail later, the observed dielectric relaxation can be attributed to the motion of only 5CB component. From Figure 7, it can be noted that the peak frequencies of two relaxation (slow and fast) modes do not change so much, but the relative intensity of the two modes changes with composition: the fast mode becomes stronger with increasing W_{5CB}.

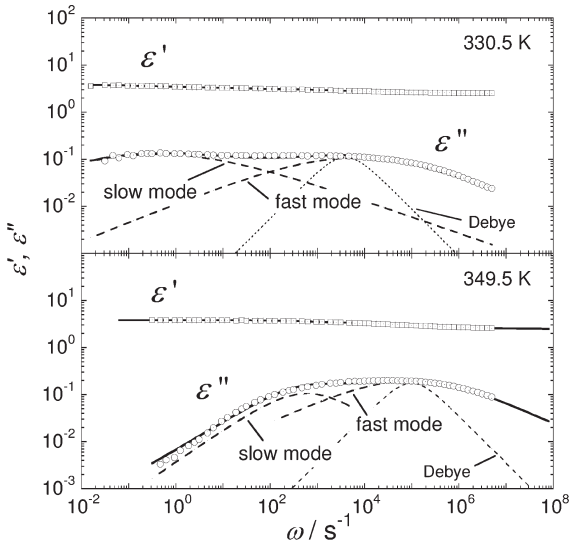

Figure 8. Typical dielectric spectra of PS/5CB mixture (W_{5CB} = 0.13) at 330.5 and 349.5 K. The solid line represents the best fitted curves obtained by using eq 6. The broken lines show the Cole−Cole function. The dotted line represents a single Debye type relaxation.

According to Onsager,[27] a dielectric relaxation intensity, $\Delta\varepsilon$ (= $\varepsilon(0) - \varepsilon_\infty$), of a polar molecule is given by

$$\frac{(\varepsilon(0) - \varepsilon_\infty)(2\varepsilon(0) + \varepsilon_\infty)}{\varepsilon(0)(2 + \varepsilon_\infty)^2} = \frac{\rho\phi N_A}{M}\frac{\mu^2}{9\varepsilon_0 k_B T} \quad (5)$$

Here, $\varepsilon(0)$ and ε_∞ are dielectric permittivities at ω = 0 and ∞, respectively, ε_0 is the electric constant (or the vacuum permittivity), N_A is Avogadro's number, and ρ is the density of the system. M and ϕ are the molecular weight and the volume fraction of a polar molecule having electric dipole moment, μ, in the mixture, respectively. The densities of PS and 5CB are almost the same (ρ_{PS} = 1.04 and ρ_{5CB} = 1.01[28] in the isotropic state); thus, ϕ can be replaced by the weight fraction, W. From eq 5, the dielectric intensities, $\Delta\varepsilon$, of PS and 5CB components in the mixtures can be estimated by using the μ values calculated by WinMopac software (Fujitsu): μ (repeating unit of PS) = 0.21 D and μ (5CB) = 4.4 D (1 D = 3.33564 × 10^{-30} C m). Thus, calculated theoretical values of dielectric intensities, $\Delta\varepsilon_{theo}$, are summarized in Table 1. $\Delta\varepsilon_{theo}$ for bulk PS (0.039) is less than 1/18 of that from 5CB in the mixture even at the lowest W_{5CB} (=0.067). This large difference in dielectric intensities indicates that the contribution of PS relaxation is negligibly small, so that only the 5CB relaxation is observed in the dielectric spectra for the mixtures. In conclusion, both the fast and slow modes in the bimodal spectra can be attributed to the relaxations of the 5CB molecule.

Figure 8 shows the dielectric spectra of PS/5CB mixture (W_{5CB} = 0.13) at 330.5 and 349.5 K. As seen in these spectra, the dielectric relaxations of the mixtures were much broader than the Debye type relaxation[29] (the single mode relaxation shown by a dotted line). Therefore, the broad dielectric spectra were fitted by the sum of the two Cole−Cole type relaxation functions[30,31] given by eq 6.

$$\varepsilon^*(\omega) = \varepsilon_\infty + \sum_{j=\text{slow, fast}} \frac{\Delta\varepsilon_j}{1 + (i\omega\tau_j)^{\alpha_j}} \quad (6)$$

Here, α_j is the symmetric broadening parameter for j mode. In the case of the Debye type function, this parameter is equal to 1. For

dx.doi.org/10.1021/ma201719c |*Macromolecules* 2011, 44, 8324–8332

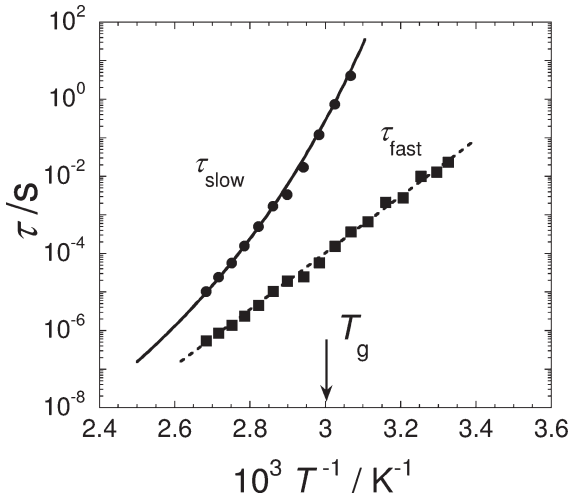

Figure 9. Temperature dependences of dielectric relaxation times, τ_{slow} and τ_{fast}, for PS/5CB mixture at weight fraction of 5CB, $W_{5CB} = 0.13$.

many glass-forming materials, in order to fit the α relaxation spectrum related to the glass transition, the Havriliak−Negami (HN) function[32] (given by eq 7) has been often used. The main reason why eq 6 instead of HN function was used is that smaller numbers of fitting parameter (α_j, $\Delta\varepsilon_j$, τ_j) compared to the HN function (α_j, β_j, $\Delta\varepsilon_j$, τ_j) minimize the ambiguity in fitting procedure. Specifically, the usage of HN function resulted in a good fit, but several combinations of α_j and β_j values were possible, and the parameters strongly depended on temperature due to the limitation of experimentally available frequency range. Additionally, eq 6 was enough to reproduce the ε^* shapes around the peak frequencies, since the purpose of this fitting was to determine the average relaxation times τ_j. For these reasons, the Cole−Cole function was used to fit the data this time. The fit curves for PS/5CB ($W_{5CB} = 0.13$) are shown by solid lines in the figure. The values of α_{slow} and α_{fast} were 0.35 and 0.33 at 330.5 K and 0.55 and 0.42 at 349.5 K, respectively. This means that the dielectric relaxation spectra of these two modes became broader with decreasing temperature, indicating the broadening of the relaxation time distribution for 5CB in the mixture. The two distinct relaxation times of 5CB in the mixture, τ_{slow} and τ_{fast}, obtained by this fit, are plotted against the reciprocal of temperature in Figure 9 (so-called the Arrhenius plot). As seen in Figure 9, τ_{slow} steeply increases in the vicinity of T_g with decreasing temperature while τ_{fast} on a logarithmic scale (log τ_{fast}) is proportional to T^{-1}: the former shows the non-Arrhenius WLF type temperature dependence given by eq 4 and the latter the Arrhenius type temperature dependence. For all other mixtures with different compositions, the τ_{slow} and τ_{fast} values were also determined and shown as functions of $T - T_g$ in Figure 10A. It can be seen that both τ_{slow} and τ_{fast} form single-universal curves in this temperature range. This suggests that the fast and slow modes of 5CB are both related to the glass transition of the mixtures.

The dielectric intensities $\Delta\varepsilon_{slow}$, $\Delta\varepsilon_{fast}$, and $\Delta\varepsilon_{total}$ (= $\Delta\varepsilon_{slow}$+ $\Delta\varepsilon_{fast}$) obtained from the fitting procedure with eq 6 are summarized in Table 1. It is noted that $\Delta\varepsilon_{total}$ and $\Delta\varepsilon_{theo}$ values are similar, meaning that both slow and fast modes are related to the rotational relaxation of 5CB. Furthermore, the similarity of $\Delta\varepsilon_{total}$ and $\Delta\varepsilon_{theo}$ indicates that 5CB molecules are well dispersed in the mixture without dipole−dipole correlation, denying the formation of dimers or other higher order aggregates,

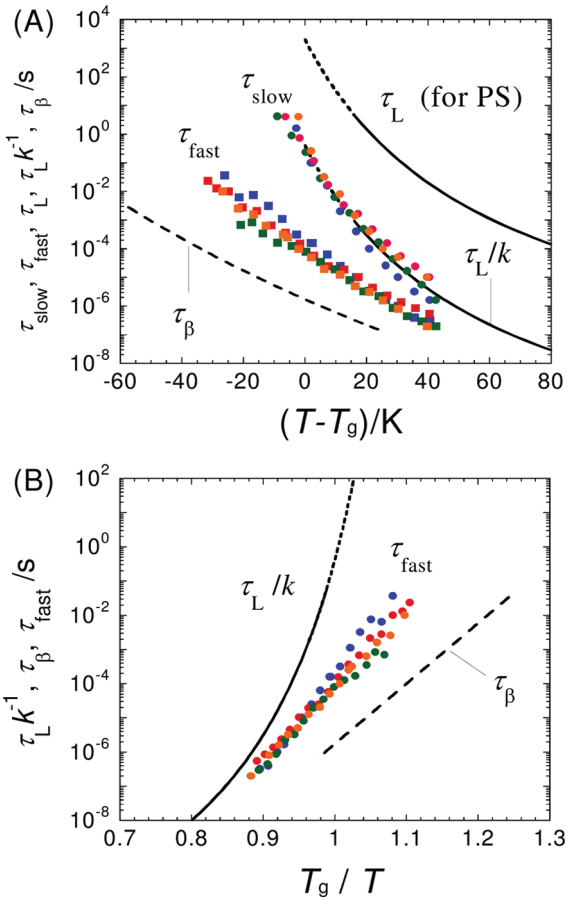

Figure 10. (A) Temperature dependence of three relaxation times, τ_{slow}, τ_{fast}, and τ_L for PS/5CB mixtures at various compositions. Blue, red, green, and orange symbols correspond to $W_{5CB} = 0.067$, 0.13, 0.19, and 0.27, respectively. The factor $k = 5000$ was used to superpose the viscoelastic relaxation time τ_L/k to the τ_{slow}. This k value is larger than the square of the Rouse mode number ($19^2 \approx 360$). The dashed line shows β relaxation time of bulk PS, τ_β, taken from the literature data.[40] (B) Temperature dependence of τ_{fast}, τ_L/k, and τ_β, which were plotted against T_g/T.

which change the effective dipole moment of 5CB molecule. From the $\Delta\varepsilon$ data shown in Table 1, it is noted that the relative intensities of the slow and fast modes depend on W_{5CB}.

3.4. Relaxation Mechanism of 5CB in PS/5CB Mixtures. As described in the previous section, two relaxation modes (slow and fast modes) were observed in dielectric spectra for PS/5CB mixtures, and both modes could be attributed to the rotational motion of 5CB. Now, the detailed relaxation mechanisms for these two modes will be discussed. It is obvious that the concentration fluctuation (CF) effect makes the relaxation time distribution broad but cannot give bimodal distribution. Therefore, the observed bimodal relaxation spectra cannot be explained by the CF effect. Concerning the possibility that two kinds of 5CB species having the slow and fast relaxation times exist in PS/5CB mixtures, two cases can be considered: (1) phase separation and (2) formation of small aggregate of 5CB, like dimer, trimer, etc., due to dipole−dipole interactions. Hori et al.[23,33] reported that the two components in the PS/5CB mixture are homogeneously mixed within the composition range studied here, so that the mixtures did not undergo phase separation. Therefore, the possibility (1) of phase separation was excluded. The possibility

(2) of the formation of small aggregates of 5CB molecules was also denied from the discussion in the previous section concerning the dielectric intensity based on eq 5. From these considerations, it is reasonable to think that the motion of a 5CB molecule takes place in two steps which correspond to slow and fast processes as suggested by Urakawa et al.[12]

Since rotational relaxation times of a rodlike molecule such as 5CB around long and short axes are known to be different,[34,35] there will be a possibility that these two modes correspond to the fast and slow modes. However, the dielectric intensity of the rotational motion around long axis is very small in the isotropic state. Therefore, this assignment will not be correct. From these viewpoints discussed above, the previously made assignment, i.e., the slow and fast modes correspond to the rotation of whole 5CB molecule coupled with the α relaxation of PS and fluctuation (wobbling) motion of 5CB permitted in a restricted free space by the less mobile PS chains, seems to be reasonable at this point. In the next section, the relaxation times of the slow and fast modes are compared with the PS chain relaxation to consider the 5CB dynamics in more detail.

3.5. Comparison of the Dielectric and Viscoelastic Relaxation Times. In Figure 10A, we showed that the slow relaxation time, τ_{slow}, had the WLF type T dependence, expressed by a universal function of $T - T_g$. This means that the slow mode of 5CB has a strong correlation with glass transition phenomena of the PS/5CB mixtures. In general, glass transition is related to the segmental motion (α relaxation) of polymer chains and the relaxation time at T_g becomes 1−100 s.[36] Since τ_{slow} at T_g takes about 1 s (cf. Figure 10A), the slow mode of 5CB around T_g has the same order of time scale with the α relaxation of PS.

In order to compare the component dynamics, the terminal relaxation time, τ_L, which is related to the global motion of PS chain, is also shown in Figure 10A along with τ_{slow} and τ_{fast}. The temperature dependence of τ_{slow} seems to be similar to that of τ_L although the time scale of τ_{slow} is about 3 orders shorter than τ_L. To compare them more clearly, τ_L curve is vertically shifted downward by multiplying a numerical factor k^{-1}. By setting k = 5000, the τ_L/k could be superposed to the τ_{slow} in the T range of $T > T_g + 20$ K as shown in Figure 10A. This means that the slow mode of 5CB is cooperative with the PS chain motion. Since the global (viscoelastic) relaxation time of polymers is known to have the same T-dependence with the segmental relaxation time at high temperatures ($T > T_g + 20-30$ K),[37−39] it can be considered that the segmental dynamics of PS is dominating the slow mode of 5CB component.

To examine the meaning of k (=5000), it is interesting to compare τ_L/k with the fastest Rouse relaxation time in eq 3, τ_N (N is the number of the Rouse segments), which is considered to be in the same order with the dielectric segmental relaxation times. The fastest Rouse mode corresponds to $p = N$ in eq 3 and can be regarded as a fundamental process for the global chain motion of polymers. Inoue et al. determined the molecular weight corresponding to the Rouse segment, M_s, for PS to be 850 from a rheo-optical method.[41,42] By using this M_s value, N for PS in this study ($M_w = 1.59 \times 10^4$) is estimated to be 18.7. This gives the relaxation time of the fastest mode, $\tau_{seg(Rouse)}$ ($= \tau_L/N^2$) = $\tau_L/350$, which is longer than τ_{slow} ($= \tau_L/5000$). From this comparison and the same T dependence of τ_L and τ_{slow}, it can be concluded that, while the slow mode of 5CB reflects the smaller scale motion than the Rouse segment, the fundamental dynamic process for these two types of motion is the same in the temperature range of $T > T_g + 20$ K.

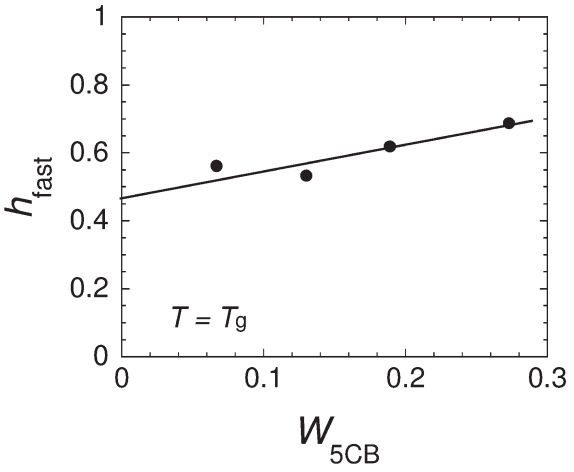

Figure 11. Fraction of dielectric relaxation intensity for the fast mode h_{fast} as a function of W_{5CB}.

In contrast, T dependence of the fast mode is obviously different from that of the PS chain motion as shown in Figure 10A,B. This indicates that the fast mode is not cooperative with the PS chain dynamics. In the previous studies,[12,19,43] the fast mode was considered to be the spatially restricted motion of 5CB in a "cage" mainly formed by PS matrices. Since the fast mode is uncooperative with the α-motion of PS, it is natural that the temperature dependence of τ_{fast} will obey the Arrhenius equation: $\tau = \tau_0 \exp(E_a/RT)$. Here, R is the gas constant, τ_0 is the relaxation time at limiting high temperature, and E_a is the activation energy. In Figure 10B, τ_{fast} data for all the PS/5CB mixtures are plotted against T_g/T. It seems that all the data can be approximately represented by a single straight line, meaning that the activation energy is almost proportional to T_g. This suggests that the fast mode is related to the free volume fraction, which may have the connection with the degree of the spatial restriction for the fluctuation motion of 5CB. The activation energies, $E_{a(fast)}$, determined from the slope of the straight line were 120−180 kJ mol^{-1}, which are summarized in Table 1. These energies are 3−6 times larger than that of the rotational motion for 5CB in the pure and isotropic state (30−40 kJ mol^{-1}),[44] which was determined by a dielectric measurement. Therefore, the fast mode of 5CB is not a free rotational motion like in isotropic liquid but strongly affected by the existence of PS chain. The spatial scale of the constraint for the 5CB motion should be smaller than the segment size of PS, since the fast mode is not directly driven by the segmental motion of PS.

Yano and Wada[40] reported that dielectric β relaxation of bulk PS obeyed the Arrhenius equation and had the activation energy, $E_{a(\beta)}$, of 126 kJ mol^{-1}. The energy is in the same order of the activation energies of the fast mode in PS/5CB mixtures. The similarity of E_a for τ_{fast} and τ_β suggests that the fast mode of 5CB may have the similar activation process with the β relaxation of PS. Although the mechanism of the β relaxation was speculated to be the local fluctuation motion of the backbone chain of PS, the actual motional unit of the β relaxation is not specified. As seen in Figure 10A,B, τ_{fast} is longer than τ_β, indicating that the fast mode has larger dynamical scale than the β relaxation of PS. As mentioned in Table 1, $E_{a(fast)}$ is a slight decreasing function of W_{5CB}, suggesting that the fast mode would not be coupled with the β relaxation of PS because E_a of β relaxation is considered to be independent of W_{5CB}. The fast mode of 5CB may be rather governed by the size of free space which

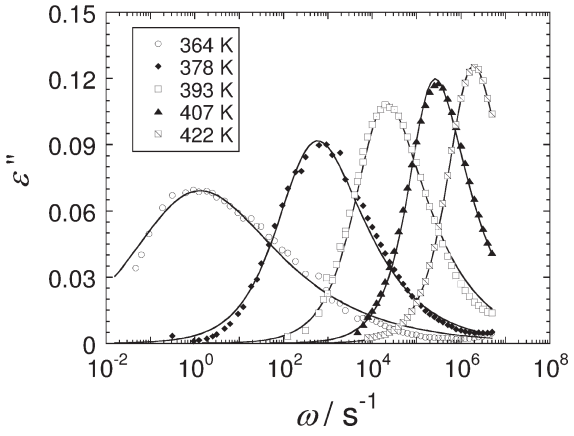

Figure 12. Comparison of dielectric spectra for PS/5CT mixture (W_{5CB} = 0.04) at several temperatures. The solid lines are best fitted results by using eq 7.

induces the wobbling motion of 5CB molecules, and the $E_{a(fast)}$ will be determined by the local free volume size.

The fraction of the dielectric relaxation intensity for the fast mode, defined as $h_{fast} = \Delta\varepsilon_{fast}/(\Delta\varepsilon_{fast} + \Delta\varepsilon_{slow})$, is calculated to be 0.56, 0.74, 0.77, and 0.82 for W_{5CB} = 0.067, 0.13, 0.19, and 0.27, respectively, at T_g + 20 K from the values shown in Table 1. Therefore, the relative intensity of the fast mode increases with increasing the concentration of 5CB compared at $T = T_g$, as seen in Figure 7 and also in Table 1. Since the intensity of the fast mode reflects the amplitude of the fluctuating motion of 5CB under the restriction of the cage formed by PS matrix, the increase of h_{fast} suggests that the cage size around 5CB molecule increases with W_{5CB}. Figure 11 shows the W_{5CB} dependence of h_{fast}. From the extrapolation of h_{fast} to W_{5CB} = 0, it can be seen that fast mode of 5CB does not disappear at infinite dilution. This means that a cage with a certain size around 5CB molecule is created even at infinite dilution for PS/5CB mixtures.

3.6. Dielectric Relaxation of 5CT in PS/5CT Mixtures. Figure 12 shows dielectric loss spectra of PS/5CT mixture at W_{5CT} = 0.04. In contrast to the spectrum shapes of PS/5CB shown in Figure 6, those of PS/5CT mixture are apparently unimodal and sharper. As previously reported,[12,19] the isochronal ε'' curves as functions of temperature more clearly showed the unimodality of the relaxation time distribution for PS/5CT mixtures. The reason why the ε'' curves apparently become unimodal was explained by the suppression of the fast mode for PS/5CT system; i.e., the wobbling motion in a restricted cage becomes difficult for the large-size 5CT molecule. In more detail, there will be a critical length, l_c, for the apparent disappearance of the wobbling motion: l_c will be in between the lengths of the long axis of 5CB and 5CT molecules. With increasing temperature, the peak position shifts to the higher frequency side and the shape of ε'' curves become narrower. Since the Cole−Cole function given by eq 6 could not perfectly fit these spectra shown in Figure 12 due to the asymmetry in the shape of the ε'' curves, the Havriliak−Negami function[32] given by eq 7 was used instead of eq 6 to fit the data.

$$\varepsilon^*(\omega) = \varepsilon_\infty + \frac{\Delta\varepsilon}{(1 + (i\omega\tau_{HN})^\alpha)^\beta} \quad (7)$$

Here, τ_{HN} is the characteristic relaxation time and β is an extra parameter to represent the degree of asymmetry of the spectrum shape.

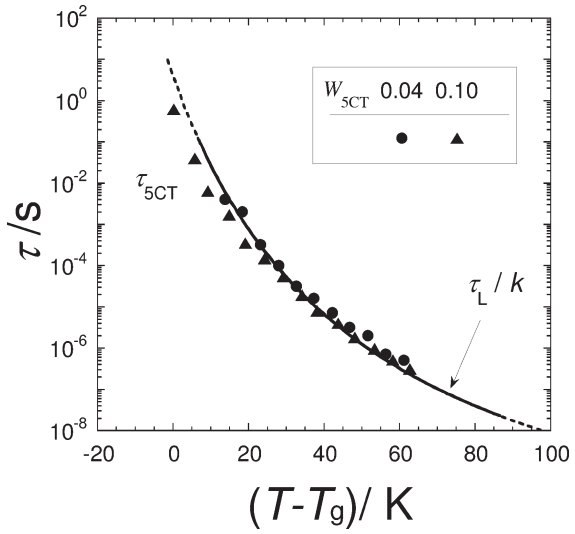

Figure 13. Temperature dependence of relaxation time τ_{5CT} for PS/5CT mixtures (W_{5CB} = 0.04 and 0.10). The solid line represents the τ_L/k data with k = 2000. The dashed line is the WLF function with c_1 = 13 and c_2 = 50 K at the reference temperature, $T_r = T_g$.

The fit curves are also shown by solid lines in Figure 12. The obtained parameters α and β were 0.45 and 0.60 at 364 K and 0.95 and 0.55 at 407 K, respectively. β did not change so much but α decreased with decreasing temperature, meaning the relaxation time distribution became narrower with increasing temperature without changing the symmetry of the ε'' curves. The relaxation intensities, $\Delta\varepsilon$, were obtained to be 0.37 and 0.75 for PS/5CT mixtures of W_{5CT} = 0.04 and 0.11, respectively, from the fit of the data with eq 7. These intensities are close to $\Delta\varepsilon_{theo}$ (0.31 and 0.95 for W_{5CT} = 0.04 and 0.11, respectively) estimated by eq 5 with the dipole moment of 5CT (μ_{5CT} = 4.8 D), meaning that each 5CT molecule is well dispersed in PS matrices without aggregation in the same way with 5CB.

It is known that the relaxation time in the Havriliak−Negami function, τ_{HN}, does not correspond to the peak frequency, in the case of $\beta \neq 1$. The relaxation time, τ_{max}, representing the peak frequency is given by the following equation:[45]

$$\tau_{max} = \tau_{HN}\left[\frac{\sin\left(\frac{\pi\alpha\beta}{2(\beta+1)}\right)}{\sin\left(\frac{\pi\alpha}{2(\beta+1)}\right)}\right]^{1/\alpha} \quad (8)$$

From this equation, the average relaxation time of 5CT, τ_{5CT} (=τ_{max}), was determined and plotted against $T - T_g$ in Figure 13. The viscoelastic relaxation time divided by k, τ_L/k (here we set k = 2000 to superpose them), for PS/5CT mixtures are also compared in this figure. It is seen that the temperature dependence of τ_{5CT} is the same with that of τ_L, at least $T > T_g$ + 20 K, indicating that the rotational motion of 5CT is cooperative with the PS component dynamics. By comparing τ_{5CT} with τ_{slow} (for 5CB) which is shown in Figure 10, the k factors were different: 2000 and 5000 for 5CT and 5CB, respectively. This difference will be explained in the following section.

3.7. Time Scale of Cooperative Motion for 5CB and 5CT. The relaxation times of 5CB and 5CT in the mixtures compared at the same $T - T_g$ were slightly different: τ_{5CT} is 2.5 times longer than τ_{slow} of 5CB (the values of k for 5CT and 5CB are

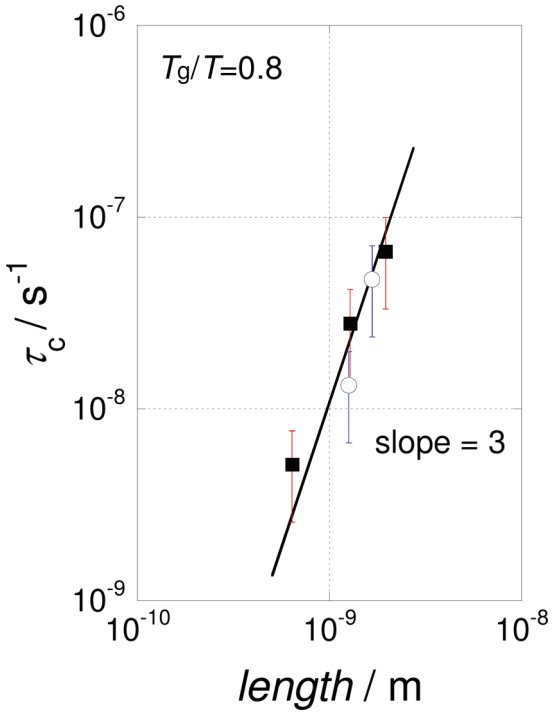

Figure 14. Relationship between the length of long axis and the cooperative relaxation time, τ_c, of LMs dissolved in PS matrix at T_g/T = 0.8. The open circle represents the data in this study. The closed squares show the literature data reported by van den Berg et al.[21] The cooperative relaxation time is proportional to the cube of the length, indicating the validity of eq 9 in the PS/LM systems.

2000 and 5000, respectively, as explained in Figures 10 and 13). The difference in relaxation times is considered to be due to a difference in molecular sizes. By regarding 5CB and 5CT molecules as cylinder shapes, the rotational relaxation time, τ, can be estimated by the following equation (rotational relaxation time for a rod in continuum media).[34]

$$\tau = \frac{\pi\eta L^3}{6k_B T(\ln(L/d) - \gamma)} \quad (9)$$

Here, η is the viscosity coefficient of the media and, L and d are the length of the long and short axes for the rod. γ is a correction factor concerning the hydrodynamic interaction between rods.[34] The value is determined to be 0.8, based on the point force approximation. Since 5CB and 5CT have flexible pentyl group attached to the rigid bi- or terphenyl groups, eq 9 is not applicable in a strict sense. However, assuming that the fluctuation and rotation of the pentyl chain around the long axis of bi- or terphenyl group is much faster than the rotational motion of whole molecules, the contribution of the pentyl group to the total length of the cylinder-like molecule can be approximately calculated by using the freely rotating chain model. The calculated average lengths of the long axis were 1.26 and 1.67 nm for 5CB and 5CT, respectively, and the ratio, τ_{5CT}/τ_{slow}, became 2.3, which was very close to the experimental value of 2.5. Furthermore, eq 9 predicts that the rotational relaxation time, τ, is approximately proportional to the cube of the rod length, L, i.e., $\tau \propto L^3$. Figure 14 shows the relationship between the LM length and the cooperative relaxation time, τ_c, at $T_g/T = 0.8$ for PS/5CB and PS/5CT mixtures along with the reported data for other LMs (derivatives of benzene, stilbene, and 1,4-bis(*trans*-styryl)-benzene) dissolved in PS matrix.[21] Despite the difference in chemical structures of LMs, all τ's seem to show a single straight line with slope 3 as shown in Figure 14; that is, the $\tau \propto L^3$ dependence given by eq 9 holds for PS/LM systems. This result indicates that the difference in the relaxation time is due to the size difference of low-mass molecules irrespective of the LM structures. Furthermore, it can be said that the dynamics of LMs are governed by the same effective viscosity coefficient (η in eq 9). The η value can be roughly estimated to be about 10^{-1} Pa s, being much smaller than that of typical glass-forming materials at $T = 0.8T_g$: $10-10^9$ Pa s which strongly depend on the material's fragility.[5] This means that the LM motion in PS matrix is not governed by the macroscopic viscosity corresponding to the glass mode but by a local viscosity which is lower than the macroscopic one.

4. CONCLUSION

In this study, the component dynamics in the mixtures of two rodlike low-mass molecules (4-pentyl-4′-cyanobiphenyl (5CB) and 4-pentyl-4′-cyanoterphenyl (5CT)) and polystyrene (PS) were examined by using dynamic viscoelastic relaxation (VR) and dielectric relaxation (DR) measurements. Temperature dependence of the viscoelastic terminal relaxation time, τ_L, of the mixtures reflecting the global motion of PS could be represented by a single WLF equation by choosing the reference temperature $T_r = T_g$. Viscoelastic relaxation spectra for all PS/5CB and PS/5CT mixtures could be fitted by the Rouse model; the relaxation time distribution in the terminal region did not change so much with the composition.

The PS/5CB mixture exhibited two rotational relaxation (slow and fast) modes in the DR spectra, both corresponding to 5CB motion, while PS/5CT mixture exhibited one rotational mode of 5CT. By comparing the temperature dependences of the rotational relaxation times of 5CB and 5CT in the mixtures with that of τ_L reflecting the PS chain dynamics in the mixture, it was concluded that the rotational motions of 5CB (slow mode) and 5CT were cooperative with the α dynamics of PS chain. In particular, the cooperative relaxation time of the low-mass molecules was found to be proportional to the cube of the length (long axis) for the molecules as predicted by the theory for rodlike molecules in a continuous medium. On the other hand, the fast mode in PS/5CB mixtures attributed to the fluctuation of 5CB in a restricted free volume (or a cage) showed the Arrhenius type T-dependence with activation energies of 120−180 kJ mol^{-1}. The relaxation intensity of the fast mode depended on both temperature and composition which might change the cage size.

AUTHOR INFORMATION

Corresponding Author

*E-mail: nobukawa@jaist.ac.jp (S.N.), urakawa@chem.sci.osaka-u.ac.jp (O.U.).

Present Addresses

†School of Materials Science, Japan Advanced Institute of Science and Technology, Nomi, Ishikawa 923-1292, Japan.

ACKNOWLEDGMENT

This work was partly supported by the Osaka University Global COE program, "Global Education and Research Center

for Bio-Environmental Chemistry", from the Ministry of Education, Culture, Sports, Science, and Technology, Japan, by Grant-in-Aid for Scientific Research B from the Japan Society for the Promotion of Science (Grants 1806809, 20340112, and 21350126), and by the Sasakawa Scientific Research Grant from the Japan Science Society (Grant 21-350).

REFERENCES

(1) Fox, T. G.; Flory, P. J. *J. Polym. Sci.* **1954**, *14*, 315–319.
(2) Adam, G.; Gibbs, J. H. *J. Chem. Phys.* **1965**, *43*, 139–146.
(3) Cangialosi, D.; Alegria, A.; Colmenero, J. *Phys. Rev. E* **2007**, 76.
(4) Ferry, J. D. *Viscoelastic Properties of Polymers*, 3rd ed.; Wiley: New York, 1980.
(5) Angell, C. A. *J. Non-Cryst. Solids* **1991**, *131*, 13–31.
(6) Inoue, T.; Cicerone, M. T.; Ediger, M. D. *Macromolecules* **1995**, *28*, 3425–3433.
(7) Roland, C. M.; Ngai, K. L. *J. Non-Cryst. Solids* **1994**, *172*, 868–875.
(8) Kanaya, T.; Tsukushi, T.; Kaji, K.; Bartos, J.; Kristiak, J. *Phys. Rev. E* **1999**, *60*, 1906–1912.
(9) Hirose, Y.; Urakawa, O.; Adachi, K. *Macromolecules* **2003**, *36*, 3699–3708.
(10) Hirose, Y.; Urakawa, O.; Adachi, K. *J. Polym. Sci., Part B: Polym. Phys.* **2004**, *42*, 4084–4094.
(11) Ellison, C. J.; Mundra, M. K.; Torkelson, J. M. *Macromolecules* **2005**, *38*, 1767–1778.
(12) Urakawa, O.; Ohta, E.; Hori, H.; Adachi, K. *J. Polym. Sci., Part B: Polym. Phys.* **2006**, *44*, 967–974.
(13) Colmenero, J.; Arbe, A. *Soft Matter* **2007**, *3*, 1474–1485.
(14) Zheng, W.; Simon, S. L. *J. Polym. Sci., Part B: Polym. Phys.* **2008**, *46*, 418–430.
(15) Olson, B. G.; Srithawatpong, R.; Peng, Z. L.; McGervey, J. D.; Ishida, H.; Maier, T. M.; Halasa, A. F. *J. Phys.: Condens. Matter* **1998**, *10*, 10451–10459.
(16) Runt, J. P.; Fitzgerald, J. J. *Dielectric Spectroscopy of Polymeric Materials*; American Chemical Society: Washington, DC, 1997.
(17) Adachi, K.; Fujihara, I.; Ishida, Y. *J. Polym. Sci., Part B: Polym. Phys.* **1975**, *13*, 2155–2171.
(18) Yoshizaki, K.; Urakawa, O.; Adachi, K. *Macromolecules* **2003**, *36*, 2349–2354.
(19) Urakawa, O.; Nobukawa, S.; Shikata, T.; Inoue, T. *Nihon Reoroji Gakkaishi* **2010**, *38*, 41–46.
(20) Watanabe, H.; Urakawa, O. *Korea-Australia Rheol. J.* **2009**, *21*, 235–244.
(21) van den Berg, O.; Wubbenhorst, M.; Picken, S. J.; Jager, W. F. *J. Non-Cryst. Solids* **2005**, *351*, 2694–2702.
(22) Hains, P. J.; Williams, G. *Polymer* **1975**, *16*, 725–729.
(23) Hori, H.; Urakawa, O.; Adachi, K. *Polym. J.* **2003**, *35*, 721–727.
(24) Rouse, P. E. *J. Chem. Phys.* **1953**, *21*, 1272–1280.
(25) Ferry, J. D.; Landel, R. F.; Williams, M. L. *J. Appl. Phys.* **1955**, *26*, 359–362.
(26) McCrum, N. G.; Read, B. E.; Williams, G. *Anelastic and Dielectric Effects in Polymeric Solids*; Dover Publications, Inc.: New York, 1967.
(27) Onsager, L. *J. Am. Chem. Soc.* **1936**, *58*, 1486–1493.
(28) Zgura, I.; Moldovan, R.; Beica, T.; Frunza, S. *Cryst. Res. Technol.* **2009**, *44*, 883–888.
(29) Debye, P.; Ramm, W. *Ann. Phys.* **1937**, *28*, 0028–0034.
(30) Cole, K. S.; Cole, R. H. *J. Chem. Phys.* **1941**, *9*, 341–351.
(31) Alvarez, F.; Alegria, A.; Colmenero, J. *Phys. Rev. B* **1991**, *44*, 7306–7312.
(32) Havriliak., S.; Negami, S. *Polymer* **1967**, *8*, 161–210.
(33) Nobukawa, S.; Urakawa, O.; Shikata, T.; Inoue, T. *Zairyo* **2009**, *58*, 47–52.
(34) Doi, M.; Edwards, S. F. *The Theory of Polymer Dynamics*; Oxford University Press: New York, 1986.
(35) Kundu, S. K.; Okudaira, S.; Kosuge, M.; Shinyashiki, N.; Yagihara, S. *J. Chem. Phys.* **2008**, *129*, 164509.
(36) Kremer, F.; Schönhals, A. *Broadband Dielectric Spectroscopy*; Springer-Verlag: Berlin, 2003.
(37) Adachi, K.; Hirano, H. *Macromolecules* **1998**, *31*, 3958–3962.
(38) Roland, C. M.; Ngai, K. L.; Santangelo, P. G.; Qiu, X. H.; Ediger, M. D.; Plazek, D. J. *Macromolecules* **2001**, *34*, 6159–6160.
(39) Roland, C. M.; Ngai, K. L.; Plazek, D. J. *Macromolecules* **2004**, *37*, 7051–7055.
(40) Yano, O.; Wada, Y. *J. Polym. Sci., Part A-2: Polym. Phys.* **1971**, *9*, 669–686.
(41) Inoue, T.; Mizukami, Y.; Okamoto, H.; Matsui, H.; Watanabe, H.; Kanaya, T.; Osaki, K. *Macromolecules* **1996**, *29*, 6240–6245.
(42) Inoue, T.; Matsui, H.; Osaki, K. *Rheol. Acta* **1997**, *36*, 239–244.
(43) Nobukawa, S.; Urakawa, O.; Shikata, T.; Inoue, T. *AIP Conf. Proc.* **2008**, *1027*, 561–563.
(44) Jadzyn, J.; Czechowski, G.; Legrand, C.; Douali, R. *Phys. Rev. E* **2003**, *67*.
(45) Diaz-Calleja, R. *Macromolecules* **2000**, *33*, 8924–8924.